

## Regional differences in tropical lightning distributions

DENNIS J. BOCCIPPIO\*

STEVEN J. GOODMAN†

STAN HECKMAN‡

(17 April 2000)

### ABSTRACT

Observations from the NASA Optical Transient Detector (OTD) and TRMM-based Lightning Imaging Sensor (LIS) are analyzed for variability between land and ocean, various geographic regions and different (objectively-defined) convective "regimes". The bulk of the order-of-magnitude differences between land and ocean regional flash rates are accounted for by differences in storm spacing (density) and/or frequency of occurrence, rather than differences in storm instantaneous flash rates, which only vary by a factor of two on average. Regional variability in cell density and cell flash rates closely tracks differences in 85 GHz microwave brightness temperatures. Monotonic relationships are found with the gross moist stability of the tropical atmosphere, a large scale "adjusted state" parameter. This strongly suggests that it will be possible, using TRMM observations, to objectively test numerical or theoretical predictions of how mesoscale convective organization interacts with the larger scale environment. Further parameters are suggested for a complete objective definition of tropical convective "regimes".

## 1 Introduction

The correlations between lightning flash rates and related meteorological (storm and environmental) properties are a topic of vigorous and continuing research. Localized case studies and field campaigns have suggested diagnostic (and sometimes predictive) relationships between lightning and thunderstorm updraft growth (Goodman et al. 1988), rainfall rate (Petersen and Rutledge 1998; Tapia et al. 1998; Alexander et al. 1999), cloud top height (Williams 1985; Cherna and Stansbury 1986; Price and Rind 1992) and mesocyclone occurrence (MacGorman et al. 1989; Williams et al. 1999). A strong complication in such field campaign-based studies is that many relationships are nonrobust (or nonunique) when applied to convection from different regions. Even in the (comparatively) meteorologically "simple" convective environment of the tropics, globally invariant relationships between lightning and other observed parameters are rare.

As examples of the lack of regional invariance in such

relationships, Petersen and Rutledge (1998) computed lightning-rainfall ratios for various regions around the globe, and found local "rain yield" relationships with strong diagnostic value. However, these relationships were in some manner dependent on the local 'convective regime', presumably a mix of the frequency, vigor, depth and level of organization of local storms. Williams et al. (1992) found weak relationships between daily Convective Available Potential Energy (CAPE) values and daily lightning production for Darwin, Australia, as did Petersen et al. (1996) for the tropical west Pacific. However, Burkett and Rennó (1999) in an analysis of soundings from GATE, DUNDEE, AMEX, ABLE and Orlando field campaigns have recently found no *single* large scale relationship between characteristic CAPE values and total lightning yield, suggesting that there is an underlying regional modulation. Working in the reverse direction, Price and Rind (1992) have attempted to use IR cloud top measurements to derive proxy relationships for regional lightning rates, for use in global chemistry models. However, these relationships required at best a bifurcation into land and ocean categories in order to be useful, implying a fundamental difference in the capacity of (comparably deep) land and ocean storms to produce lightning.

These differences in land/ocean regional lightning

---

\*Corresponding author address: Dennis J. Boccippio, Global Hydrology and Climate Center, NASA / Marshall Space Flight Center, AL 35812. Email: Dennis.Boccippio@msfc.nasa.gov.

†Global Hydrology and Climate Center, NASA / Marshall Space Flight Center

‡University Space Research Association, Huntsville, AL 35806

production have recently been quantified rigorously by the NASA Optical Transient Detector (OTD) (Christian et al. 1996; Christian et al. 1999) and Lightning Imaging Sensor (LIS) (Christian et al. 1999) which have, at the time of press, mapped global and tropical lightning for five and three years, respectively. Climatological, annual regional flash rate  $f_r$  has been found to vary over at least 2 orders of magnitude across the tropics, with much of the difference found between land and ocean, but with additional variability within continental or oceanic regions, in patterns initially suggested by DMSP (Orville and Henderson 1986) lightning climatologies (Fig. 1).<sup>1</sup>

Explaining the dramatic variability in  $f_r$  evident in Fig. 1 requires understanding of:

1. Why the underlying convective spectra (meteorological properties such as updraft magnitude, ice content aloft, etc.) vary regionally
2. How these spectra map to lightning production

In this study, we attempt to make incremental advances in this effort. By examining the differences in per-storm cell lightning distributions (rather than bulk regional production), we confirm that regional variability is driven by cell density, or frequency of occurrence, a necessary first step in addressing (1) and (2) through global observation. We then examine controls other than geographic binning which might aid in more rigorously pursuing (1).

The approach is as follows: In section 2, we detail the data processing and quality control of OTD and LIS data relevant for this investigation, and in section 3 identify significant regional differences - and surprising similarities - in individual storm flash rates, frequency of storm occurrence, and observed lightning properties (optical radiance and footprint). These observations will help clarify our understanding of the wide dynamic range of observed regional flash rates.

Broad categorization into land and ocean regions, or into regional "convective regimes", serves a useful descriptive purpose but does not necessarily advance understanding of the underlying physics. A fundamental problem is that the definitions of a convective regime have to date either been poorly constrained, or largely phenomenological. In sections 4 and 5 we offer a more clearly defined framework for identifying (and quantifying) "convective regimes" across which observations may be intercompared. Specifically, we suggest that

<sup>1</sup>In the climatological data underlying Fig. 1, the most common ratio of LIS to OTD  $f_r$  is found to be 1.65. For the purposes of these plots only,  $f_r$  is adjusted by an assumed OTD flash detection efficiency  $DE_f$  of 46%, and a LIS  $DE_f$  of 75% (this maintains the 1.65 ratio). In subsequent analyses, this cross-normalization is not performed, as we are not yet confident that this adjustment is regionally invariant and wish to minimize assumption-based bias in our results.

lack of control for the magnitude and spatio-temporal variance of surface forcing (moist enthalpy flux) and adjusted atmospheric state (bulk stability) may obscure more commonly-shared underlying physics in regional intercomparisons and in local (field program) data analyses.

## 2 Methodology

The primary data sources for this study are OTD and LIS flash observations. Both sensors measure total (intracloud and cloud-to-ground) lightning with a high detection efficiency during both day and night, with little regional bias. Both sensors are deployed aboard low-earth orbiting satellites which slowly precess through the local diurnal cycle; thus aliasing of the local diurnal lightning cycle can be minimized via appropriate averaging (compositing data in multiples of 55 and 49 days, for OTD and LIS respectively).

The OTD sensor has been validated using both laboratory calibration (Koshak et al. 2000) and cross-sensor comparisons over the continental U.S. (Boccippio et al. 2000). These studies provide working estimates of the operational lightning detection efficiency (LDE), bias (minimal) and spatio-temporal accuracy. This latter diagnostic is of relevance to this study, as the validation studies indicate a nontrivial occurrence of satellite navigation drift during individual storm overpasses (the sensor was designed for large scale climatology, not storm case studies). We will thus not draw primary inferences from the OTD storm-level results, although we do note that OTD storm level parameters exhibit roughly the same characteristics as those derived from the LIS, whose host TRMM platform was designed for much higher spatial accuracy and pointing stability.

All OTD orbits have undergone a manual quality assurance inspection, and only orbits which raised no manual QA flags are considered in this study. Automatic quality flags are associated with each flash observation, including a "thunderstorm area count" (*TAC*) metric which gives the likelihood that a flash observation is true lightning and not ambient radiation noise. In this study, only flashes with  $TAC \geq 140$  are considered, a qualitatively derived threshold based on examination of many OTD orbit files [K.T. Driscoll, *pers comm*, 1997].<sup>2</sup> Second-to-second satellite viewing information are included in the OTD dataset, and this "viewtime" information is explicitly included in regional flash rate estimates (this is especially important for the later years

<sup>2</sup>The *TAC* metric is found in the *QA[0]* field of OTD-format HDF files, or in the *density\_index* field of OTD files translated to LIS-format HDF. The threshold value of 140 is the same as that used in the validation study of Boccippio et al. (2000).

of OTD data, during which satellite and sensor dropouts increased). During the period of study, OTD land CG lightning detection efficiencies are estimated as 46-60% for the period 7/20/95-10/23/96, and 55-70% for the period 10/24/96-present (Boccippio et al. 2000). Based on the climatological intercomparison of Fig. 1, these estimates may be slightly high biased; this is contingent on the true LIS  $DE_f$ , which is still under investigation. OTD flash rates reported in the results below do *not* include a detection efficiency adjustment, as we wish to include as few *a priori* assumptions about sensor performance over unvalidated ocean regions in these results as possible.

Validation studies of the LIS sensor are still in progress. The LIS was designed with a higher sensitivity than the OTD, and thus the OTD detection efficiency estimates serve as a lower limit on operational LIS LDE. Early estimates suggest that the LIS LDE may exceed the OTD LDE by about 15-25% over land. Preliminary intercomparisons with other sensors find the LIS spatial accuracy good to about 6 km, and stable over the course of individual overpasses (e.g., (Thomas et al. 2000)). LIS data used in this study are from the preliminary (version 4.0) release, in which there are known limitations in the data processing algorithms. Specifically, there is some indication that flashes (collections of contiguous optical pulses) may be fragmented (overcounted) by approximately 10-15%, and that some artefact (noise) filters may be overly active. These algorithms are in the process of revision and tuning, and a final dataset will soon be reprocessed and released. As with OTD, data used in this study are thus not scaled for detection efficiency, and offsets will exist between OTD and LIS estimates of some parameters presented below. As with OTD, all LIS orbits undergo manual quality inspection and contain embedded viewing information; these data are incorporated into the statistics below similarly for both OTD and LIS.

For storm level parameters, the OTD and LIS "area" products are used to identify individual cells. Areas are geographic loci of contiguous optical flashes observed during individual OV-1 (OTD) or TRMM (LIS) overpasses (Christian et al. 2000). The median and mean spatial extents of a LIS area are about 525 and 700  $km^2$  (i.e., about 26-30 km diameter). Areas represent, loosely, local regions of bulk charge separation within larger cloud systems; visual inspection of OTD/LIS areas suggests they most closely resemble individual "cells" in upper level radar reflectivity CAPPIs or 85 GHz passive microwave maps (which exhibit local features at comparable scales). As such, we will refer to area-derived products as "cell" level statistics, with the understanding that this nomenclature is no more or less arbitrarily specified

than when derived from data from more conventional sensors, and equivalently resolution-limited. The intrinsic LIS 4 km pixel resolution effectively precludes any examination of significantly smaller scale features.

Regional flash rate  $f_r$ , distributions of both per-cell flash rates  $f_c$  (number of flashes per minute in a cell during an individual overpass) and inter-cell spacing  $r_c$  (distance from each cell to its nearest neighbor) are computed from four and nearly two years of OTD and LIS data (5/1/95-4/30/99 and 12/1/97-9/30/99, respectively).<sup>3</sup> Cell density  $d_c$  is approximated as  $r_c^{-2}$ . Additionally, distributions of individual flash properties are computed; these include total flash optical radiance  $R_f$  and optical footprint  $A_f$  (area). Flash optical properties observed by the OTD and LIS represent a convolution of both the actual flash optical output and the multiple scattering attenuation arising from propagation through the cloud to cloud top. As such, regional differences in these distributions represent differences either in basic flash energetics or in cloud microphysical properties; since both types of differences are plausible, the actual source of variability is not determinable from OTD/LIS observations alone.

Radiances reported in the original OTD dataset were calculated using a crude calibration technique, assigning different sensor gain levels to three solar conditions (day, night, twilight); this technique and the resulting high radiance variance is described in Boccippio et al. (2000). Optical footprints were not included in the distributed data. As such, these parameters were rederived for OTD observations using the improved methodology included in the LIS production code. For radiances, the sensor gain was better approximated by fitting characteristic background scene radiances (upon which actual gain depends, and which are recorded only intermittently during routine data collection) to a cosine curve of the solar zenith angle (Fig. 2). This approach yields up to a 50% reduction in computed flash radiance variance (uncertainty) (Fig. 3). Flash optical footprints are computed by geolocating and overlaying the footprints of each sensor pixel event (optical pulse) in a flash. Since the OTD and LIS pixel resolutions vary by a factor of two and sensitivities differ, there will be offsets in the magnitude of these parameters between the two sensors (more dim pixels are observable by LIS, hence total radiances will be larger).

In section 3, lightning parameters are subdivided into various (tropical) geographic regions to demonstrate regional variability. These include regions identified by Mohr et al. (1999) for analysis of the spectrum of MCS 85 GHz microwave brightness temperatures; this is per-

<sup>3</sup>Hereafter, parameter symbols will be subscripted with  $r$ ,  $c$  or  $f$  to denote regional-, cell-, and flash-level parameters.

haps the best comprehensive survey of differences in tropical convective spectra available to date. Mohr et al. (1999) found significant differences in the distributions of MCS  $T_b$  for regions including the Congo Basin, Sub-Saharan Africa, Central America, India/Southeast Asia, the Amazon Basin, the Maritime Continent, Atlantic, West Pacific, Central Pacific and South Pacific Convergence Zone (SPCZ). For consistency, we follow precisely the subsetting criteria used in that study, limiting analysis based on latitude/longitude bounds, land/ocean status and wet season periods specified in their Table 1. We also present bulk estimates for revised versions of some of their definitions, including a land-only Central America bin, a land-only Maritime Continent bin, and an Amazon bin for the "less monsoon-like" months of Oct, Nov, Dec. Other categories include the GATE and TOGA/COARE domains for the months of those field programs, and bulk annual estimates for the three main tropical continental regions using a stricter land/ocean mask which eliminates "coastal" regions (Fig. 4). The regional definitions are summarized in Table 1.

In section 4, lightning parameters are analyzed against a continuously varying meteorological parameter, the climatological gross moist stability computed from 10 years (1980-1989) of ECMWF data by Yu et al. (1998). This parameter is a physically-based metric rooted in the quasiequilibrium theory of moist convective dynamics put forth by Neelin and Yu 1994; Neelin 1997, and is briefly described in section 4;  $2.5 \times 2.5$  deg gridded fields were kindly provided by Chia Chou and David Neelin and rectified to the OTD/LIS analysis grids. During analysis, we apply the same "region of applicability" masks used by Yu et al. (1998) to analyze only the 'continuously convecting' tropical regions in which their quasiequilibrium theory is assumed to hold. This analysis is not intended to suggest a direct causal relationship between gross moist stability and lightning rates, but rather to demonstrate that criteria other than simple geographic masking may plausibly be used to examine differences in realized convective spectra (as measured through the resulting lightning flash rates) across different "regimes". Section 5 examines what additional variates might be necessary to further define or constrain a convective "regime" definition in a physically-based context.

### 3 Observed regional differences

#### a. Regional differences in storm cell properties

Motivated both by the dramatic land/ocean differences in  $f_r$  evident in OTD and LIS climatologies, we have computed complete distributions (spectra) of  $f_r$ ,  $f_c$ ,  $d_c$ ,

$R_f$  and  $A_f$  for various subregions of the tropics. As discussed in section 2, we use both the regional definitions of Mohr et al. (1999) and a more restrictive (but overlapping) regional definition more exclusive of transitional coastal areas. Mohr et al. (1999)'s results are particularly instructive, as they reveal systematic differences in the spectrum of realized deep and organized (MCS) convection across the tropics (illustrated in Fig. 5). Further, preliminary analyses by Driscoll 1999; Toracinta and Zipser 1999; Toracinta and Zipser 2000 find fairly strong correlations between total lightning flash rates and TMI 85 GHz  $T_b$ , both high resolution trackers of deep convective cores; we thus might expect cell-level statistics derived from lightning observations to be matched in microwave brightness temperature cells (although such an analysis is not performed here).

Fig. 6a,b further quantifies the order-of-magnitude differences in regional flash rate production  $f_r$  between the tropical continents and oceans shown above in Fig. 1. Following the "conventional wisdom" that oceanic storms have weaker updrafts and hence weaker storm flash rates, we might expect similar order-of-magnitude differences in the per-cell flash rates  $f_c$  characteristic of the various regions. Fig. 7,8, suggest that this is not the case. These illustrate the climatological occurrence of OTD and LIS areas (area rate density), and the climatological ratio of  $f_r$  to area rate density (i.e., mean flashes per area). While the area rate density varies over nearly two orders of magnitude in patterns nearly identical to  $f_r$ , the spatial variability of bulk flashes-per-area is much smaller and this parameter explores a much narrower dynamic range. Fig. 9 further emphasizes this;  $\bar{f}_c$  (here, the mean per-cell flash rate, not the climatological bulk mean) in cells observed to flash by LIS varies by only a factor of two or so. Alternatively, the characteristic cell density  $\bar{d}_c$  varies over a large dynamic range (Fig. 10), and it is evident that *differences in large scale  $f_r$  climatologies are as much (if not more) due to the frequency of electrified cell occurrence than to the flash rates in individual cells* (i.e., when lightning producing cells occur over the tropical oceans, their flash rates do not differ as dramatically as might be expected). This could be viewed as evidence in support of the critical velocity (for lightning occurrence) hypothesis of Zipser (1994). We also note that this result has been partially corroborated by Williams et al. (2000) using a completely different cell counting technique, and was indirectly inferable from the results of Toracinta and Zipser (1999).

The above bulk differences can be further illustrated by examining the probability distributions of LIS-observed flash rates over land and ocean. To interpret these, it is important to remember that the LIS effectively has a minimum detectable flash rate  $f_{c_{min}}$  based

on its finite observation time  $\delta t$  (typically 80-90 seconds) and flash detection efficiency  $DE_f$  (about a factor of 1.65 greater than the OTD  $DE_f$ , and *preliminarily* estimated at 0.75 from the (small sample size) case study of Thomas et al. (2000)). While  $f_{c_{min}}$  is inherently probabilistic (discrete observations of 1 flash in  $\delta t$  may arise from a variety of true  $f_c$ , given that interflash intervals are not uniform), a discrete estimate can be made as:

$$f_{c_{min}} \sim \frac{1}{(\delta t)(DE_f)} \quad (1)$$

or approximately 1 fl/min. Limiting consideration of LIS-observed cells to those observed between 80-90 seconds (85% of all cells) to guarantee approximately evenly sampled discrete probability estimates, the land and ocean  $f_c$  PDF's are shown in Fig. 11a. These again are the distributions only of cells flashing at rates approximately greater than 1 fl/min. As noted above, the distributions are remarkably similar. Estimates of the population of deep cells flashing at rates below  $f_{c_{min}}$  (or not flashing at all) are of course not possible using LIS data alone. However, Nesbitt et al. (2000) have used TRMM TMI and PR data to identify deep precipitation features with significant ice scattering, and find that 50% of these are not observed by LIS to flash over land, 98% over ocean (these are thus upper bounds on the frequency of truly nonflashing cells). While there is a definitional mismatch between Nesbitt et al. (2000)'s precipitation features and LIS areas, this provides a preliminary estimate of the population of deep cells with  $f_c < f_{c_{min}}$  (and possibly 0), and allows preliminary normalization of the truncated PDFs of Fig. 11a to complete PDFs. The normalized spectra are shown in Fig. 11b, which again emphasizes that land/ocean  $f_r$  differences seem driven by differences in the probability of flashing cell occurrence, rather than differences in the  $f_c$  of significantly flashing cells.

#### b. Regional differences in flash optical properties

Fig. 12,13 present regional differences in metrics derived from the optical properties of observed flashes, flash radiance  $R_f$  and flash footprint  $A_f$ . There is clearly a tendency for oceanic cells and flashes to *appear* larger to the OTD and LIS sensors, and for the observed flashes to appear brighter. As noted in section 2, this could be due to either systematic differences in flash energetics or cloud optical depth. There is indirect evidence to consider systematic differences in flash energetics a possibility: higher dipole moment change flashes are a known feature of other low-flash rate clouds (midlatitude winter storms (Brook et al. 1982), midlatitude trailing stratiform regions (Boccippio et al. 1995)). There is also rea-

son to believe there are systematic differences in cloud optical depth between land and ocean; oceanic clouds have been reported to be comparatively depleted in supercooled liquid water (Black and Hallett 1986). These possibilities can not be deconvolved with the data used in this study. Possible methods of attacking the problem may involve estimates of flash energetics from ELF or VLF long range waveform data, and of estimation of cloud optical depth through inversion of other TRMM observables.<sup>4</sup>

#### 4 Comparison with gross moist stability

The results of section 3 help confirm significant regional differences in realized deep convective spectra first rigorously identified by Mohr et al. (1999), while adding some key new information (i.e., that there appear to be systematic differences in the spatial density (frequency) of electrified deep convective cores, and that individual cell flash rates do not, on average, vary as dramatically as the regional flash production). However, these analyses are still limited by the use of arbitrary geographic binning of the results, and do not necessarily contribute to our understanding of *why* the realized convective spectra differ. At best they identify alternate lightning observables ( $f_c, d_c$ ) which are better tied to the cellular convective physics than regional totals. To better understand the underlying physics, we should examine the lightning data in the context of continuously varying observables more directly linked to the convection itself.

One category of such observables might be global estimates of conditional instability or stability of the atmosphere. We have noted above that previous attempts to identify regionally invariant relationships between traditional measures of conditional instability (CAPE) and lightning have met with little or no success. Even if conditional stability necessarily varied with lightning activity, the specific CAPE metric awkwardly mixes the effects of high frequency surface forcing, instantaneous measurements of a continuously evolving boundary layer adjustment, and low frequency upper atmospheric adjustment; we shall return to this idea in section 5. In this section, we instead consider a metric which characterizes the upper atmospheric "adjusted state" on long (seasonal or longer) time scales. This is the gross moist stability  $M$  of the (continuously convecting regions of the) tropical atmosphere, as defined and com-

<sup>4</sup>The possibility that cloud optical depths may vary measurably between land and ocean also opens the possibility that OTD/LIS detection efficiencies have a spatial bias as well (OTD detection efficiency has only, to date, been validated over land). However, the OTD land validation results suggest that sensor DE is already quite high, thus limiting the magnitude of any further spatial bias considerably.

puted by Yu et al. (1998) from 10 years of ECMWF data.  $M$  is defined as the difference between the dry static stability  $M_s$  and the gross moisture stratification  $M_q$ , and is largely driven by subsaturation in large scale moist static energy profiles (Neelin 1997).

Gross moist stability is by no means necessarily the optimal metric for this purpose, or even one that we expect *a priori* to have a causal relationship with lightning production. Rather, it was selected for several key reasons:

1. It is a continuously varying quantity which in some way helps define a "convective regime".
2. It is rooted in a basic theory of tropical convective dynamics, which stipulates that continuously convecting regions reach a state of quasiequilibrium over appropriately long time scales. (The definition of QE adjustment is specifically restricted to the context of large scale dynamics.)
3. It is valid only for such long time scales, and thus mitigates the impact or relevance of convective modulation by higher frequency "external" (non-local) tropical dynamical disturbances.
4. It is comparatively decoupled from boundary layer processes and high frequency surface forcing (Yu et al. (1998) note that it does not vary consistently over the oceans with SST); as we will argue in section 5, it makes physical sense to quantify (control for) variability in forcing and response separately.

The primary purpose of analyzing lightning against a parameter such as  $M$  is thus simply to determine whether systematic differences might be found in realized convective spectra (as observed through lightning) which covary with a continuously varying meteorological property over global scales. This is a sharp departure from regional intercomparisons, as the independent variable in this case could point us directly to underlying physics rather than to implicit and unspecified geographic cofactors.

As a link to the discussion in section 3, Fig. 14 shows the  $M$  values characteristic of the various tropical regions and regimes of Fig. 5,6,9,10,12 and 13.<sup>5</sup> Some similar variability is evident, with high stabilities found over the open oceans and lower stabilities over the continents, although the regional variability is not as system-

atic.<sup>6</sup> When lightning properties are binned against the continuously-varying  $M$ , surprisingly stable mean relations are found. Fig. 15a shows the mean regional flash rate  $f_r$  of all 2.5 x 2.5 degree OTD and LIS composites (monthly and annual) plotted against their equivalent gross moist stabilities (monthly and annual). While there is considerable scatter in the grid cell by grid cell  $f_r$  vs  $M$  values (not shown), on average the regional flash rate decreases monotonically with increasing moist stability, and does so smoothly over nearly two orders of magnitude of realized  $f_r$ . Note that there is considerable agreement between the OTD and LIS dependencies, suggesting that details of cell identification algorithms (which vary between OTD and LIS) are of secondary importance. Fig. 15b extends this analysis by separating grid cells into land and ocean domains. This separation is somewhat instructive: First, it reveals that most of the signal in Fig. 15a is dependent upon a transition from mostly-land to mostly-ocean grid locations. Second, it demonstrates a residual correlation *within* the land and ocean domains of  $f_r$  and  $M$ , with a stronger signal manifest over oceans. Third, it indicates that a given gross moist stability (atmospheric adjusted state) may apparently be obtained through at least two characteristic convective spectra (as indirectly measured through the lightning regional flash rates). Together, these suggest that a "free troposphere" adjusted state parameter such as  $M$  is insufficient (alone) to describe the detailed nature of the convective release spectrum which achieves it. This is not particularly surprising, as we have completely ignored surface forcing (beyond implicit differences in the land/ocean categorization), but not necessarily intuitive either.

Fig. 16a,b and 17a,b extend this analysis to include cell density  $d_c$  and flash rate  $f_c$ . As in the regional statistical analyses, it is clear that most of the tenfold or greater differences in  $f_r$  are due to comparable differences in  $d_c$ , with only a small contribution from mean  $f_c$ ; further, these parameters follow gross moist stability distributions in much the same way as  $f_r$ , with wider dynamic ranges over ocean than over land. The pairing of multiple (land and ocean) values of  $d_c$  with single  $M$  states again emphasizes that different convective spectra may yield comparable adjusted states, at least as measured by  $M$ . The overall impression is that there are "missing variates" needed to unify the picture.

It is not immediately obvious why a large scale, ad-

<sup>5</sup>Because Mohr et al (1999) defined their subregions/subperiods according to local wet seasons, few locations within their subregions failed the "continuously convecting" criteria used by Yu et al (1998).

<sup>6</sup>Note that we should not, *a priori*, expect the metrics to correlate exactly. We do not contend that measures of the adjusted state should covary precisely with measures of the realized convective spectrum; indeed, since controls for surface forcing have not been considered, we should expect some unexplained variability (absence of strict covariance). We shall return to this idea in Section 5.

justed state parameter such as  $M$  should covary coherently with measures of the instantaneous spectrum of deep convective release such as lightning. To shed some light on this, it will be useful to return to the theory from which  $M$  derives, namely the quasiequilibrium framework in which 'continuously convecting' regions of the tropics attain a local adjusted state on seasonal or longer time scales. Zeng and Neelin (1999) succinctly summarize this QE response as:

$$mC = R_t - F_s \quad (2)$$

Here, net moisture convergence  $C$  is in balance with the top of the atmosphere radiative flux  $R_t$  and net surface flux  $F_s$ , and modulated by  $m$ , which can loosely be interpreted as an 'efficiency' factor. Zeng and Neelin (1999) note that  $m$  is mathematically equivalent to 'precipitation efficiency' terms framed by Emanuel et al. (1994). They describe  $m$  as a "highly lumped parameter absorbing all the effects involved in subgrid-scale moist convective processes, including mesoscale effects" ... i.e., it is the aggregate effect of the actual, realized dynamic convective spectrum. Further, within this framework,

$$m \equiv \frac{M}{M_q} \quad (3)$$

i.e.,  $m$  varies directly with  $M$ , adjusted for the gross moisture stratification. While we have not directly analyzed the lightning parameters against  $m$ , spot computation from maps presented in Yu et al. (1998) suggest that the spatial distributions of  $m$  and  $M$  are coarsely similar, and hence we expect a strong lightning/ $m$  relationship as well.

This is a fairly important result. The theoretical 'efficiency of forced moisture convergence' term  $m$  is directly diagnosable from large scale analyzed fields. It has direct (mathematical) analogues in several related theoretical frameworks for understanding tropical convective adjustment. It is *intended* to account for the ensemble effects of 'subgrid' scale convective release, and indeed it appears to covary directly with the lightning distributions (an indirect measure of these convective spectra). Neelin (1997) notes (our comments in brackets):

"The definition of  $M$  does not alone tell us why cancellation [between adiabatic cooling and convective heating] occurs in this proportion [i.e., the regional variability in  $M$ ] - since it must be set at small scales, this is left as a challenge for cloud and mesoscale modelers. It is my hope that  $M$  can provide them a quantitative target in thinking about the ensemble effects of convection."

The current demonstration shows that at least some TRMM observables of the dynamic convective spectrum (the flashing cell density (spacing) and intensity (some function of the updraft rate)) vary with  $M$ , and probably  $m$ . While this behavior is not *a priori* expected, it is consistent with the intent and meaning of the parameters (especially  $m$ ). More importantly, it shows that Neelin's challenge to cloud and mesoscale dynamicists - to formulate the ways in which local convective organization interact with the large scale environment - would be empirically testable using TRMM data or analogous modeling results.

As noted above, gross moist stability was selected simply as a convenient free tropospheric parameter with which to demonstrate continuous and monotonic variability in observed lightning properties. Unlike strict geographic binning, the use of a meteorological parameter closely tied to convection (and rooted in theory) at least allows us to place the ambiguous measurement of convective spectrum properties by lightning in a broader context. In addition to showing the physical links discussed above, our intent is also to illustrate that  $M$  (or some other metric of the free tropospheric state) is *one plausible continuous parameter which should be controlled for* in lightning (or other convective spectrum) intercomparisons at large spatial and long time scales. This concept is elaborated upon in section 5, and additional key parameters are suggested.

## 5 Discussion

In section 4 we explored one possible variable (atmospheric gross moist stability,  $M$ ) which might enter into an objective and continuously-varying parameter space in which to describe a "convective regime". We reemphasize that the purpose of even attempting to identify such regimes is to better explain - and understand - the exact nature of the spectrum of realized convection, and its relationship to indirect observables such as  $f_r$ , microwave  $T_b$ , radar reflectivity  $Z_e$ , etc. The ideal regime definition would contain controls for all major sources of variability in this spectrum, and further arbitrary (geographic or phenomenological) categorization would be unnecessary - in a sense, such a definition would provide a "unified framework" within which to intercompare tropical convection, and its large scale effects. Most importantly, such a definition could reveal important new variates needed to train convective parameterizations, numerical models and satellite retrievals to generate regionally plausible realizations of conditional instability release which are robust against changes in either high or low frequency external forcing.

This may seem to be a daunting task, but we can fall

back on basic convective physics to provide a skeletal framework. Consider a simple fluid tank laboratory convection experiment. To fully describe such an experiment, we might plausibly seek to quantify the forcing, the dynamics of the resulting internal convection, and the bulk properties of the "adjusted" fluid if the experiment is run to equilibrium.<sup>7</sup> Furthermore, if the forcing is nonstationary in space or time, we might also wish to quantify its spatial and temporal variance, in addition to its mean rate.

In the (continuously convecting) tropical atmosphere, there are obvious direct analogues to this breakdown. At the most fundamental level, surface forcing is simply the net moist enthalpy (surface sensible and latent heat) flux - a quantity which we already know has some geographic variability in its mean rate, and significant local variance both spatially and temporally, especially over land. The dynamics of the resulting internal convection *are* the realized convective spectra which we quantify indirectly through IR,  $T_b$ ,  $Z_e$ ,  $f_c$ ,  $d_c$  or a host of other observables. The bulk properties of the "adjusted" fluid *could* be described on appropriately long temporal and large spatial scales with a parameter such as  $M$ , or other appropriate thermodynamic or radiative measures of the internal properties of the free troposphere. This "three-pronged" parameter space is illustrated schematically in Fig. 18.

Clearly this framework is not new, and there have been prior attempts to implement it. In particular, CAPE is a widely used metric which purports to capture both surface forcing *and* upper atmospheric state. Indeed, CAPE is a rigorously defined and useful measure of the maximum *instantaneous* conditional instability of a point location. However, precisely because it convolves a local, instantaneous (and often poorly resolved in horizontal, vertical and temporal coordinates) measurement of a partial response of the boundary layer to surface forcing with an upper atmospheric profile in an instantaneous state of adjustment, we should not be surprised that it fails miserably to describe the bulk (large spatial and long time scale) properties of a given region, in any kind of quantitatively robust or regionally intercomparable sense. Returning to the laboratory tank analogy, it would be a peculiar design to choose to quantify the surface forcing by (infrequently) measuring the enthalpy of a particular locus of the fluid's surface sublayer and turbulent interior just above the sublayer, all of which were in the process of adjustment. This would be even

more suspect if the surface forcing contained strong spatial and temporal variability. Clearly there are observational constraints which drive researchers to investigate CAPE, but these constraints should in no way warrant surprise when high CAPEs are measured over oceanic regions with dramatically different realized convective spectra than continental regions.

At this point, we return again to the recent results of Burkett and Rennó (1999) (hereafter, BR). Having found little relationship between CAPE and total lightning, they hypothesize (within the context of the heat engine characterization of convection put forth by Rennó and Ingersoll (1996)) that the characteristic "overturning" scales of convective circulations are at least as important in determining convective updraft velocities as the magnitude of the forcing itself. Specifically, they hypothesize that surface variability over land will constrain circulations to smaller spatial scales, with concomitantly higher vertical velocities than over oceans. From this, two items bear some comment. First, it is clear that CAPE measurements alone give no unique information about the spatial variance of the surface forcing (and resulting constraints on circulation scales, if BR are correct). Second, we note that BR's prediction of smaller scale circulations is at least qualitatively consistent with our finding of significantly higher flashing cell density over tropical land than over tropical ocean (and, indirectly with the brightness temperature spectra reported by Mohr et al. (1999)). If such cell spacing differences were confirmed with other sensors (e.g., TMI, PR, which do not have the low flash rate truncation problems of LIS), this would provide significant support for - and constraints on - the BR hypothesis.

We conclude by speculating that surface moist enthalpy forcing - both its magnitude *and* spatio-temporal variance - is the dominant "missing variate" in the convective regime description outlined above. While this was really one implicit hypothesis in prior land/ocean studies, the emphasis on spatio-temporal variability appears to be given new weight by both our current results and the inferences of BR. We additionally note that global (tropical) surface moist enthalpy flux maps are virtually nonexistent, although they could be constructed with modest spatial and temporal resolution from land surface model runs and maritime flux measurements provided by the oceanographic community. While measured or simulated surface fluxes are indeed still coupled to the boundary layer convective response, this coupling is far less dramatic than that implicit in bulk boundary layer soundings which feed traditional CAPE computation.

<sup>7</sup>We would also want to document the material properties of the fluid itself, such as viscosity and thermal conductivity, which modulate the dynamic release of instability. An atmospheric analogue might be the local available CCN or ice nuclei spectra. We will temporarily put this complication aside, as its effects cannot even begin to be isolated until we have the rest of the framework established.



## 6 Caveats: Algorithm limitations

As noted in section 2, the preliminary (v4.0) release LIS data suffers from some flaws which might call into question the algorithm-independence of these results. Re-analysis of the current results using the revised/tuned LIS flash/cell clustering and filter algorithms would help determine if this were a significant concern. Until reprocessed data is available, we can at least note the following:

1. The v4.0 LIS cell clustering algorithm does not appear to have regional (land/ocean) dependencies, as illustrated in in Fig 19, which shows the CDFs of cell footprint (area) for land and ocean regions. The land and ocean distributions are identical, suggesting that the cell clustering algorithm does not covary with  $\bar{f}_c$  (an important constraint).
2. While the v4.0 LIS flash identification (pulse clustering) algorithm may fragment truly contiguous flashes, we estimate that this is not more than a 10-15% effect, using techniques described in Boccippio et al. (2000), and in comparisons with revised algorithms [K. Driscoll, D. Mach, pers. comm, 1999]. We also have no direct evidence that this fragmentation covaries with true  $f_c$ , suggesting that bias effects from this limitation will be small.
3. The correlations of mean cell parameters with gross moist stability  $M$  (Fig. 16,17) are nearly identical for OTD and LIS, despite the fact that the two datasets employ different spatial clustering algorithms to define cells. This suggests that definitional variability due to fine details of cell identification algorithms is small compared to the wide dynamic range of geophysical variability considered here.
4. Significant features of natural variability in cell parameters (e.g., the phasing of the local diurnal cycle over land) are comparable between LIS areas and storms identified using much simpler techniques (fixed-registration grid spatial 'patches'; (Williams et al. 2000)). This again argues that different cell identification algorithms would not change the most basic results of this study.

Again, the most rigorous control for algorithm dependence would be to identify cells using a non-lightning TRMM sensor with an overlapping field-of-view, as recently done by Nesbitt et al. (2000).

## 7 Conclusions

The most important direct result of the present study is the observation that per-cell flash rates differ, *at the climatological average level*, by only about a factor of two between tropical land and tropical ocean cells. When ocean storms produce lightning, they do so at rates not dissimilar from continental storms. Consistent with the results of Williams et al. (2000), who analyzed similar data using a different cell-counting technique, we find that the bulk of the difference in regional flash rate production between land and ocean is accounted for by differences in cell spacing, or equivalently frequency of occurrence. Together, these observations might argue in favor of the critical velocity hypothesis of Zipser (1994).

We further find that the optical properties of observed lightning differ measurably over land and ocean, with flashes *appearing* brighter and larger (at cloud top) in oceanic storms. We are as yet unable to determine whether this is due to differences in the energetics of the flashes or the optical scattering properties of storm cells, or some combination of the two.

Differences are also found in the regional characteristics of the convective spectrum (as observed via lightning) between different land regions, and to a lesser extent, between different ocean regions. These differences track loosely with the "cold bias" of the microwave brightness temperatures associated with MCS' in the various regions, as reported by Mohr et al. (1999).

Analyzing the same parameters, we further find (on average) continuous variability of the realized lightning distributions when analyzed against a non-geographic meteorological variable, in this case the gross moist stability of the continuously convecting regions of the tropics. We find consistent and monotonic behavior of most lightning variables analyzed against this parameter when separated into land and ocean regions, yet find different relationships over land and ocean. Most significantly, this suggests that comparable upper atmospheric thermodynamic adjusted states can be achieved by at least two different types of underlying convective spectra, and that (unsurprisingly), a metric which describes the free troposphere alone is insufficient to identify (predict) these underlying spectra. The monotonic relationship between lightning and gross moist stability (itself closely coupled to the theoretical efficiency with which the ensemble effects of local convective release are coupled to large scale moisture convergence) suggests that cloud- and mesoscale- empirical, theoretical and modelling efforts to *predict* the small/large scale coupling can indeed be empirically tested.

These results, paired with recent hypotheses by Burdett and Rennó (1999), place added emphasis on the pos-

sible importance of the character of the surface forcing in determining the realized convective spectra, at least over large spatial and long temporal scales. In particular, our observations of dramatic differences in the density (spacing) of electrified and flashing deep convective cells gives partial and indirect credence to Burkett and Rennó (1999)'s hypothesis that surface constraints on the horizontal scales of convective circulations may couple with the intensity of these circulations. If so, then the spatial (and perhaps temporal) *variance* of the surface forcing - something often poorly specified in both numerical models and model-driven satellite retrieval techniques - may be as important as the *magnitude* of this forcing in determining the realized convective spectra. This chain of inference is highly preliminary, but the current observations suggest that further investigation into this possibility is warranted.

## 8 Acknowledgements

We thank Kevin Driscoll for invaluable discussions on this material, and for exhaustive quality analyses of the satellite data which identified restrictions on the applicability of this preliminary analysis; Dennis Buechler for tireless manual quality assurance of the OTD and LIS datasets; Steve Nesbitt for early access to results from his multisensor TRMM comparisons; Chia Chou and David Neelin for access to their gross moist stability analyses; and most importantly Earle Williams and Karen Rothkin for motivating the storm frequency of occurrence / storm flash rate investigation, and for frequent discussions on the results. We especially thank Walt Petersen for an extremely comprehensive, critical and valuable review.

## REFERENCES

- Alexander, G. D., J. A. Weinman, V. M. Karyampudi, W. S. Olson, and A. C. L. Lee, 1999. The effect of assimilating rain rates derived from satellites and lightning on forecasts of the 1993 superstorm. *Mon. Wea. Rev.*, **127**, 1433–1457.
- Black, R. A., and J. Hallett, 1986. Observations of the distribution of ice in hurricanes. *J. Atmos. Sci.*, **43**, 802–822.
- Boccippio, D. J., K. T. Driscoll, W. J. Koshak, R. J. Blakeslee, W. L. Boeck, D. A. Mach, D. E. Buechler, H. J. Christian, and S. J. Goodman, 2000. The Optical Transient Detector (OTD): Instrument characteristics and cross-sensor validation. *J. Atmos. Oc. Tech.*, **17**, 441–458.
- Boccippio, D. J., E. R. Williams, S. Heckman, W. A. Lyons, I. T. Baker, and R. Boldi, 1995. Sprites, ELF transients and positive ground strokes. *Science*, **269**, 1088–1091.
- Brook, M., M. Nakano, P. R. Krehbiel, and T. Takeuti, 1982. The electrical structure of the Hokuriku winter thunderstorms. *J. Geophys. Res.*, **87**, 1207–1215.
- Burkett, M. L., and N. O. Rennó, 1999. Related aspects of CAPE, vertical velocity and lightning frequency. *Mon. Wea. Rev.*, **submitted**.
- Cherna, E. V., and E. J. Stansbury, 1986. Sferics rate in relation to thunderstorm dimensions. *J. Geophys. Res.*, **91**, 8701–8707.
- Christian, H. J., R. J. Blakeslee, D. J. Boccippio, W. L. Boeck, D. E. Buechler, K. T. Driscoll, S. J. Goodman, J. M. Hall, W. J. Koshak, D. M. Mach, and M. F. Stewart, 1999. Global frequency and distribution of lightning as observed by the Optical Transient Detector (OTD). In *Proc. 11th International Conf. on Atmospheric Electricity* (Guntersville, AL, 7–11 June 1999 1999), pp. 726–729. ICAE.
- Christian, H. J., R. J. Blakeslee, S. J. Goodman, D. A. Mach, M. F. Stewart, D. E. Buechler, W. J. Koshak, J. M. Hall, W. L. Boeck, K. T. Driscoll, and D. J. Boccippio, 1999. The Lightning Imaging Sensor. In *Proc. 11th International Conf. on Atmospheric Electricity* (Guntersville, AL, 7–11 June 1999 1999), pp. 746–749. NASA.
- Christian, H. J., R. J. Blakeslee, S. J. Goodman, and D. M. Mach, 2000. Algorithm Theoretical Basis Document (ATBD) for the Lightning Imaging Sensor (LIS). <http://eospsa.gsfc.nasa.gov/atbd/listables.html>.
- Christian, H. J., K. T. Driscoll, S. J. Goodman, R. J. Blakeslee, D. A. Mach, and D. E. Buechler, 1996. The Optical Transient Detector (OTD). In *Proc. 10th International Conference on Atmospheric Electricity* (Osaka, Japan, 1996).
- Driscoll, K. T., 1999. A comparison between lightning activity and passive microwave measurements. In *11th International Conf. on Atmospheric Electricity* (Guntersville, AL, 7–11 June 1999 1999), pp. 523–526. ICAE.
- Emanuel, K. A., J. D. Neelin, and C. S. Bretherton, 1994. On large-scale circulations in convecting atmospheres. *Quart. J. Roy. Met. Soc.*, **120**, 1111–1143.
- Goodman, S. J., D. E. Buechler, P. D. Wright, and W. D. Rust, 1988. Lightning and precipitation history of a microburst producing storm. *Geophys. Res. Lett.*, **15**, 1185–1188.
- Koshak, W. J., J. W. Bergstrom, M. F. Stewart, H. J. Christian, J. M. Hall, and R. J. Solakiewicz, 2000. Lightning Imaging Sensor calibration. *J. Atmos. Oc. Tech.*. In press.
- MacGorman, D. R., D. W. Burgess, V. Mazur, W. D. Rust, W. L. Taylor, and B. C. Johnson, 1989. Lightning rates relative to tornadic storm evolution on 22 May 1981. *J. Atmos. Sci.*, **46**, 221–250.
- Mohr, K. I., J. S. Famiglietti, and E. J. Zipser, 1999. The contribution to tropical rainfall with respect to convective system type, size and intensity estimated from 85 GHz ice-scattering signature. *J. Appl. Met.*, **38**, 596–606.
- Neelin, J. D., 1997. Implications of convective quasi-equilibrium for the large-scale flow. In R. K. Smith, Ed., *The physics and parameterization of moist atmospheric convection*, pp. 413–446. The Netherlands: Kluwer Academic Publishers.
- Neelin, J. D., and J. Y. Yu, 1994. Modes of tropical variability under convective adjustment and the Madden-Julian oscillation. Part I: Analytical theory. *J. Atmos. Sci.*, **51**, 1876–1894.
- Nesbitt, S. W., E. J. Zipser, and D. J. Cecil, 2000. A census of precipitation features in the tropics using TRMM: Radar, ice scattering and lightning observations. *J. Clim.*, **In press**.
- Orville, R. E., and W. Henderson, 1986. Global distribution of midnight lightning: September 1977 to August 1978. *Mon. Wea. Rev.*, **114**, 2640–2653.
- Petersen, W. A., and S. A. Rutledge, 1998. On the relationship between cloud-to-ground lightning and convective rainfall. *J. Geophys. Res.*, **103**, 14025–14040.
- Petersen, W. A., S. A. Rutledge, and R. E. Orville, 1996. Cloud to ground lightning observations from TOGA COARE: Selected results and lightning location algorithms. *Mon. Wea. Rev.*, **124**, 602–620.
- Price, C., and D. Rind, 1992. A simple lightning parameterization for calculating global lightning distributions. *J. Geophys. Res.*, **97**, 9919–9933.
- Rennó, N. O., and A. P. Ingersoll, 1996. Natural convection as a heat engine: a theory for CAPE. *J. Atmos. Sci.*, **53**, 572–585.
- Tapia, A., J. A. Smith, and M. Dixon, 1998. Estimation of convective rainfall from lightning observations. *J. Appl. Met.*, **37**, 1497–1509.
- Thomas, R. J., P. R. Krehbiel, W. Rison, T. Hamlin, D. J. Boccippio, S. J. Goodman, and H. J. Christian, 2000. Comparison of ground-based 3-dimensional lightning mapping observations with satellite-based LIS observations in Oklahoma. *Geophys. Res. Lett.*, **In press**.
- Toracinta, E. R., and E. J. Zipser, 1999. Lightning and 85 GHz MCSs in the global tropics. In *Proc. 11th International Conf. on Atmospheric Electricity* (Guntersville, AL, 7–11 June 1999 1999), pp. 440–443. ICAE.
- Toracinta, E. R., and E. J. Zipser, 2000. Lightning and 85 GHz MCSs in the global tropics. *J. Appl. Met.*, **submitted**.

- Williams, E. R., 1985. Large scale charge separation in thunderclouds. *J. Geophys. Res.*, **90**, 6013.
- Williams, E. R., R. Boldi, A. Matlin, M. Weber, S. Hodanish, D. Sharp, S. J. Goodman, R. Raghavan, and D. E. Buechler, 1999. The behavior of total lightning activity in severe Florida thunderstorms. *Atmos. Res.*, **51**, 245–265.
- Williams, E. R., K. Rothkin, D. Stevenson, and D. J. Boccippio, 2000. Global lightning variations caused by changes in thunderstorm flash rate and by changes in the number of thunderstorms. *J. Appl. Met.*, **In review**.
- Williams, E. R., S. A. Rutledge, S. G. Geotis, N. O. Rennó, E. Rasmussen, and T. Rickenbach, 1992. A radar and electrical study of tropical “hot towers”. *J. Atmos. Sci.*, **49**, 1386–1395.
- Yu, J. Y., C. Chou, and J. D. Neelin, 1998. Estimating the gross moist stability of the tropical atmosphere. *J. Atmos. Sci.*, **55**, 1354–1372.
- Zeng, N., and J. D. Neelin, 1999. A land-atmosphere interaction theory for the tropical deforestation problem. *J. Clim.*, **12**, 857–872.
- Zipser, E. J., 1994. Deep cumulonimbus cloud systems in the tropics with and without lightning. *Mon. Wea. Rev.*, **122**, 1837–1851.

Symbol	Name	Lat.	Long.	L/O	Coast tolerance	Months
CG	Congo Basin	8S-5N	10E-28E	Land	loose	MAM
SS	Sub-Saharan Africa	5N-18N	18W-45E	Land	loose	JAS
CA	Central America	2N-12N	75W-85W	Both	n/a	JAS
IN	India / SE Asia	12N-35N	70E-122E	Land	loose	JJA
AZ	Amazon Basin	15S-3N	45W-75W	Land	loose	JFM
MC	Maritime Continent	15S-2N	95E-155E	Both	n/a	DJF
CP	Central Pacific	2N-12N	155E-150W	Ocean	loose	ASO
EP	East Pacific	3N-15N	90W-150W	Ocean	loose	JJA
AT	Atlantic	0N-15N	7W-50W	Ocean	loose	ASO
SP	SPCZ	35S-12S	180W-120W	Ocean	loose	JFM
CA'	Central America (land)	2N-12N	75W-85W	Land	loose	JAS
MC'	Maritime Cont. (land)	15S-2N	95E-155E	Land	loose	DJF
AZ'	Amazon Basin (break)	15S-3N	45W-75W	Land	loose	OND
GT	GATE domain	4N-20N	28W-8W	Ocean	loose	JAS
TC	COARE domain	10S-10N	140E-180E	Ocean	loose	DJF
AF	Africa	23.5S-23.5N	20W-50E	Land	strict	All
AM	Americas	23.5S-23.5N	120W-35W	Land	strict	All
MC	Maritime Continent	23.5S-23.5N	90E-160E	Land	strict	All
L	Tropical Land	23.5S-23.5N	180W-180E	Land	strict	All
O	Tropical Ocean	23.5S-23.5N	180W-180E	Ocean	strict	All

TABLE 1: Regional definitions used throughout this study. The first ten categories correspond exactly to those in Mohr et al, 1999. The next three represent "tweaked" versions of three of their categories; a land-only Central America, land-only Maritime Continent, and "non-monsoon" (Oct-Dec) Amazon rainy season. Definitions for the GATE and TOGA/COARE domains correspond to conventional geographic boundaries and the months of those campaigns. The last five categories employ a 'stricter' land/ocean separation which excludes coastal regions.

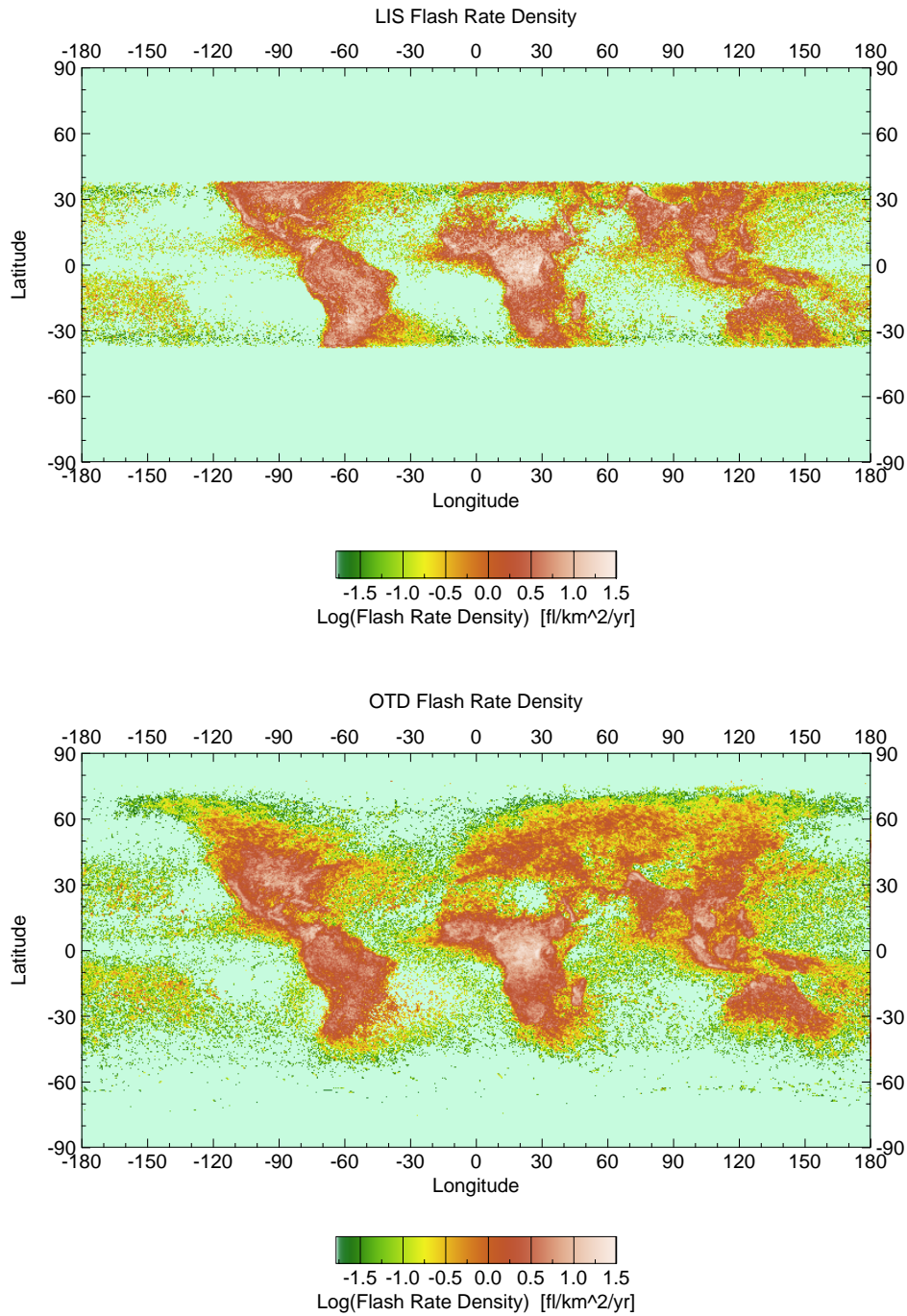


FIGURE 1: (a) Climatological LIS flash rate density  $f_r$ , Dec 1997 - Nov 1999. Data have been normalized by sensor viewtime and an assumed detection efficiency of 75%. (b) Climatological OTD flash rate density  $f_r$ , May 1995 - Apr 1999. Data have been normalized by sensor viewtime and an assumed detection efficiency of 46%.

FIGURE 2: Empirical fit of actual scene background radiance at OTD lightning "event" pixels (used in determination of instantaneous OTD/LIS sensor gain, and hence flash radiance calibration) against the cosine of the local solar zenith angle. True background radiances were taken from the subset of OTD data with coincident background scenes (these scenes are only stored approximately every 30 seconds). Background radiances B1-B6 correspond to "D/C" radiance levels used in laboratory calibration of the "A/C" pixel response (e.g., Koshak et al, 2000). Levels B1, B3 and B5 were used in the distributed OTD data to calibrate pixel radiances. The clean solar zenith angle dependence indicates that most OTD pixel events occur on high albedo clouds. The revised calibration technique used here and in the distributed LIS data estimates background radiance directly from the fitted curve (i.e., assumes high cloud albedo) and interpolates between background levels used in laboratory calibration, hence yielding a much more robust "A/C" lightning radiance estimate.

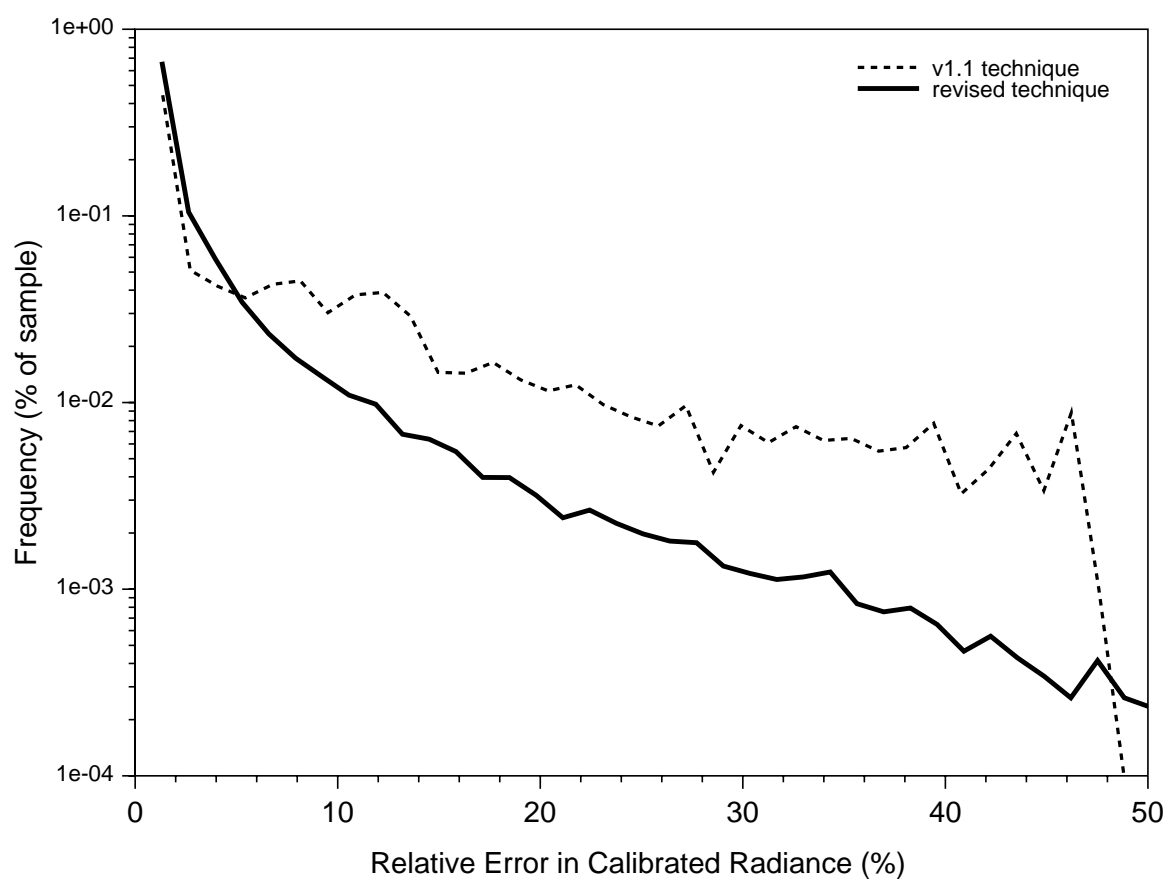


FIGURE 3: Reduction in calibrated OTD radiance uncertainty when the sensor gain level is approximated by the cosine of the solar zenith angle. This approach is used operationally in determination of calibrated LIS flash radiances.

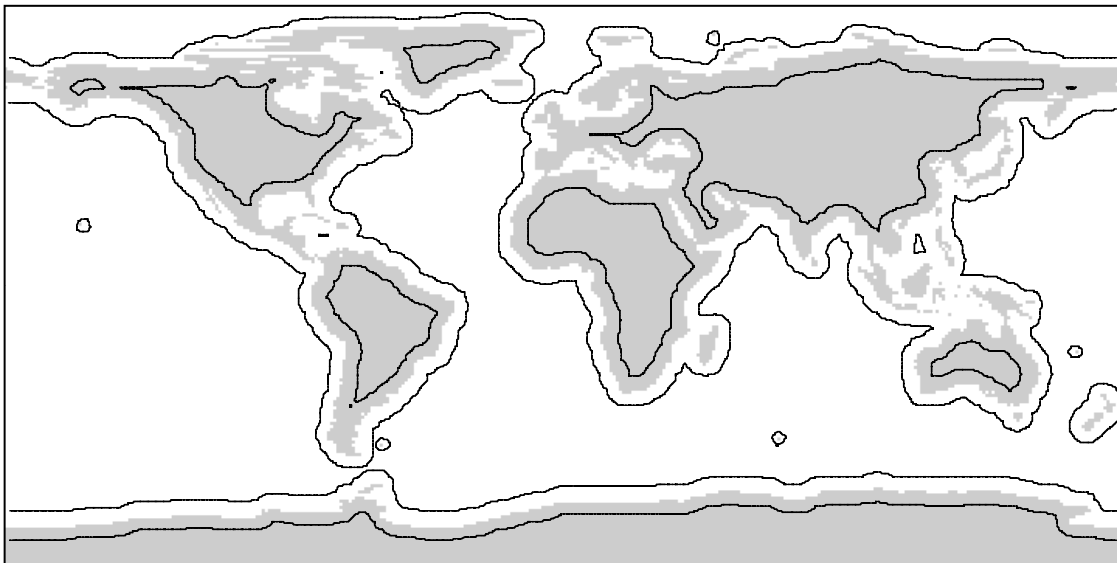


FIGURE 4: Land/ocean mask used in the "strict" separation categories of Table 1 (derived from smoothing a high resolution terrain grid).



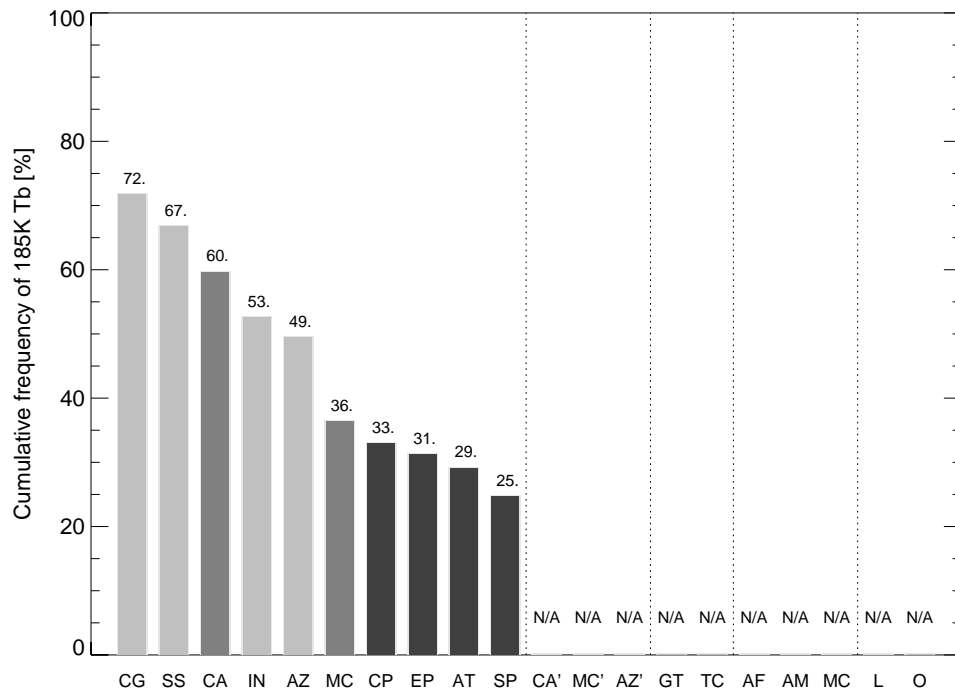


FIGURE 5: Cumulative frequency of 185K microwave brightness temperature  $T_b$  for various tropical regions' wet seasons, from Fig. 3 of Mohr et al (1999). Regions are as defined in Table 1. Light grey bars denote land-only regions, medium grey land and ocean, and dark grey ocean-only.

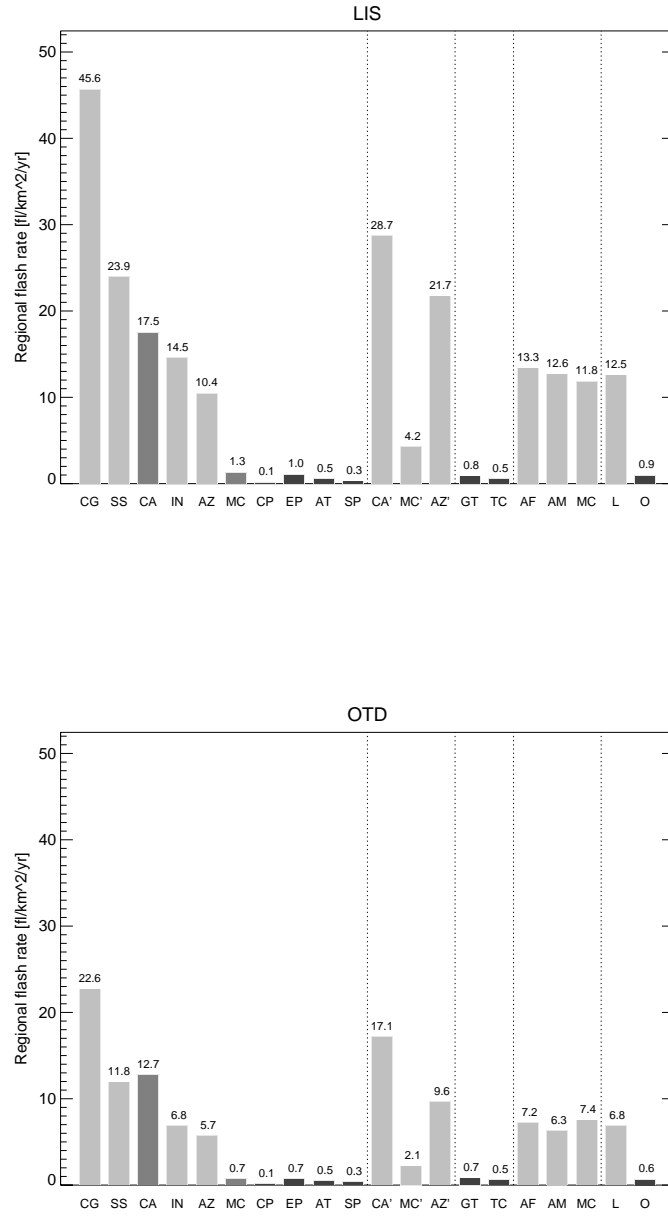


FIGURE 6: Regional flash rate  $f_r$  determined for OTD and LIS using the definitions of Table 1. Rates are *not* scaled for detection efficiency. Bar shading is as in Fig. 5.

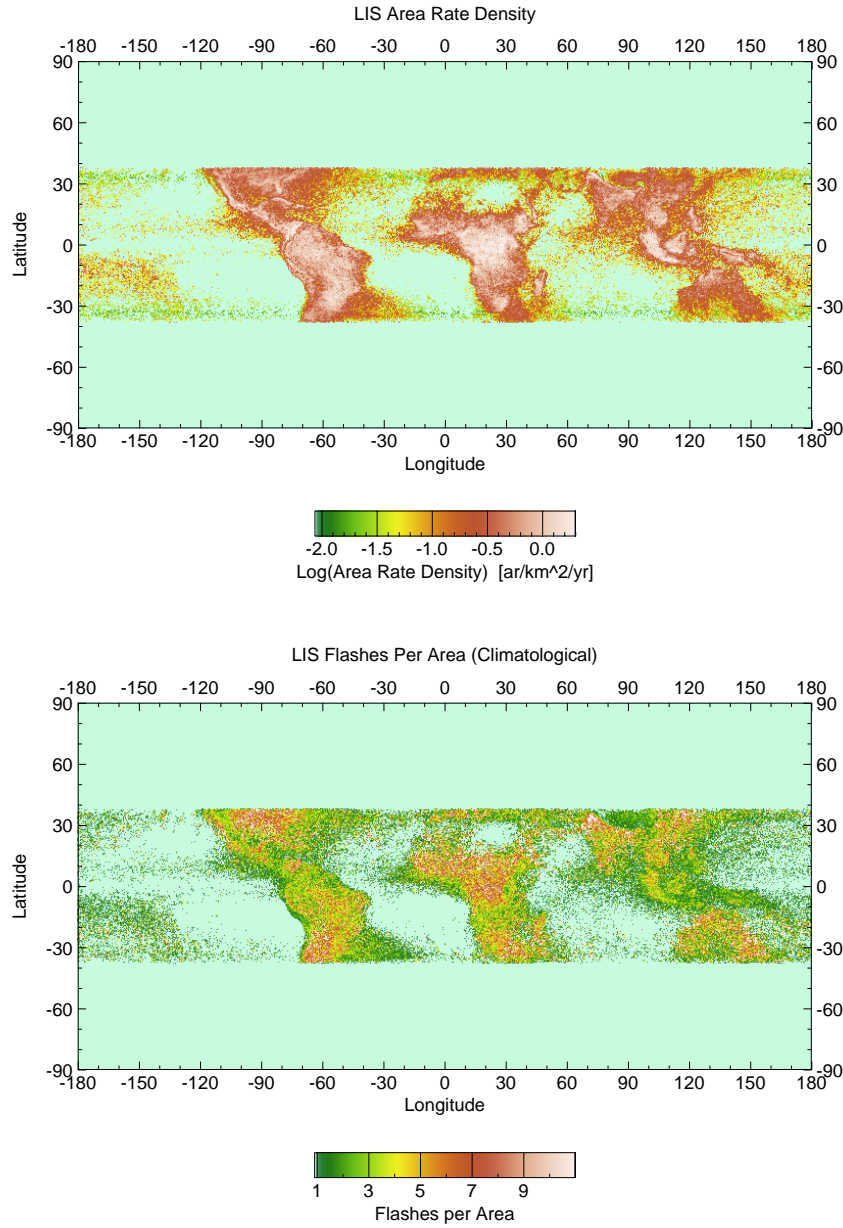


FIGURE 7: (a) Mean LIS area rate density, Dec 1997 - Nov 1999. Data are normalized by total sensor viewtime. No detection efficiency adjustment has been applied. (b) Climatological map of LIS flashes per area (i.e., regional flash rate density divided by regional area rate density). No detection efficiency adjustment has been applied.

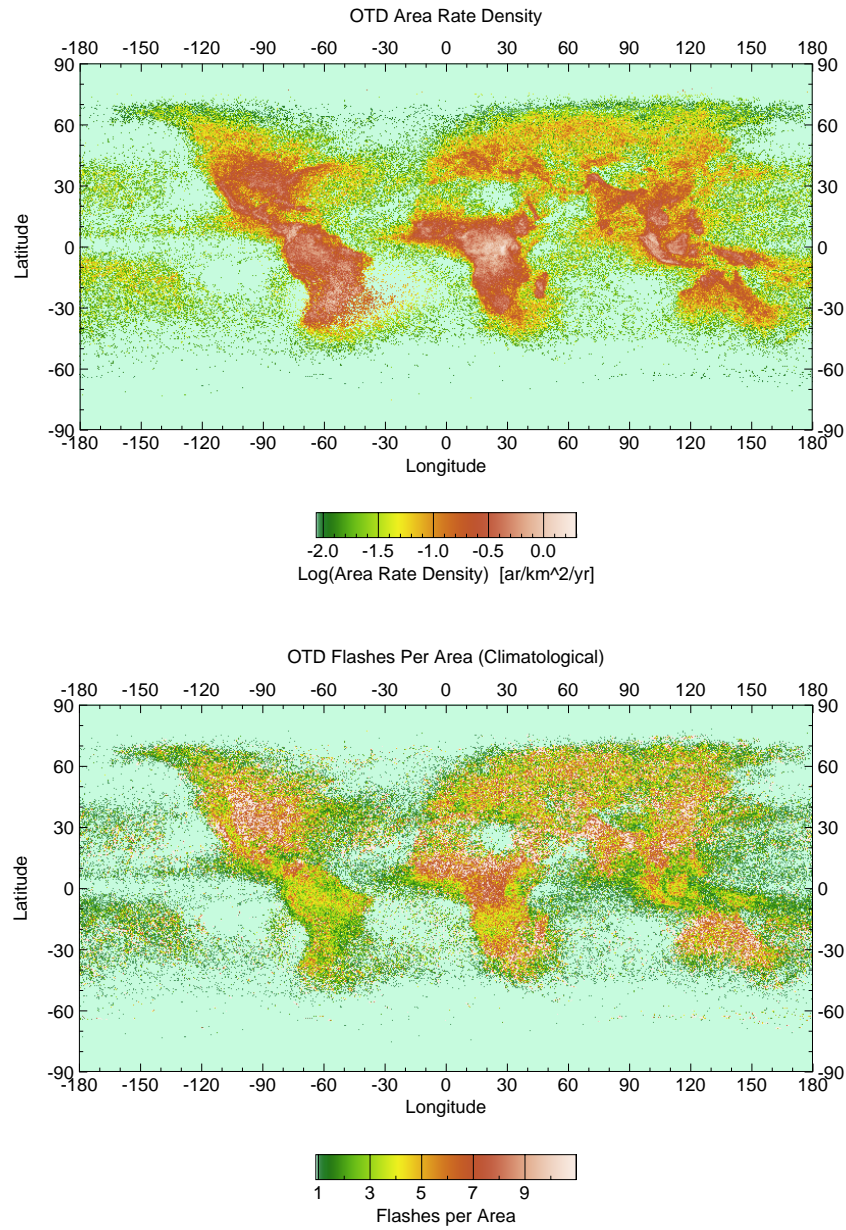


FIGURE 8: (a) Mean OTD area rate density, May 1995 - Apr 1999. Data are normalized by total sensor viewtime. No detection efficiency adjustment has been applied. (b) Climatological map of OTD flashes per area (i.e., regional flash rate density divided by regional area rate density). No detection efficiency adjustment has been applied.

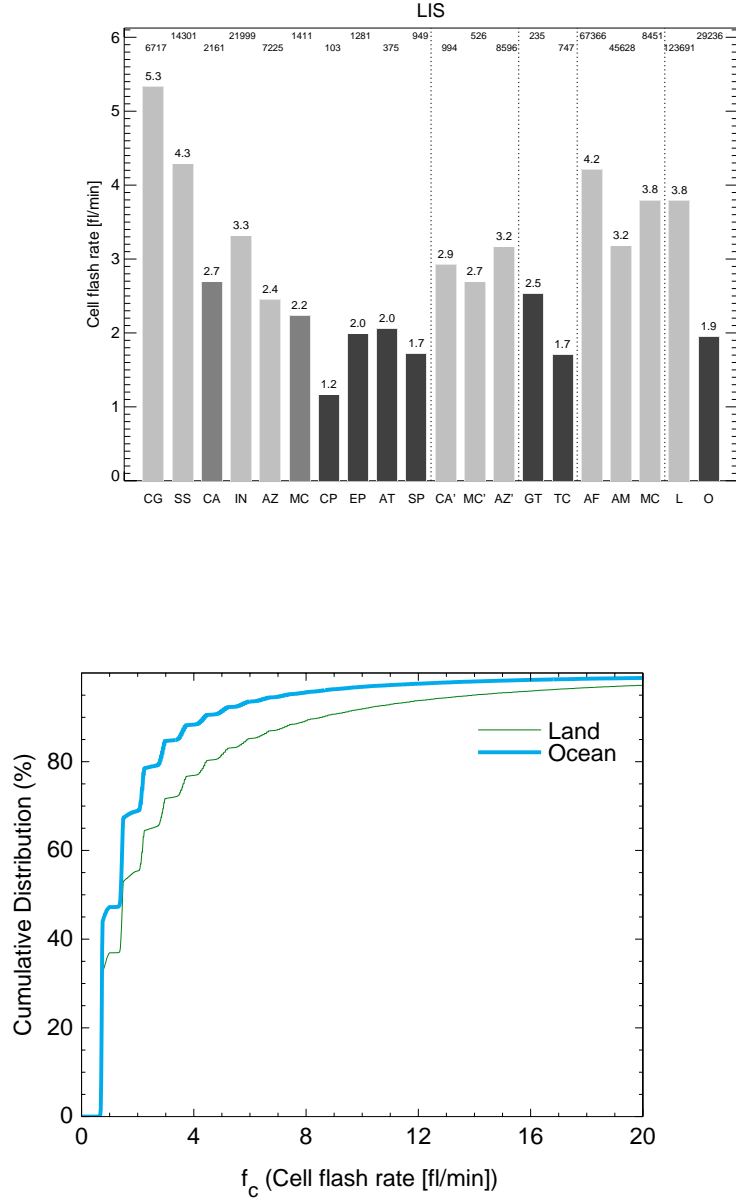


FIGURE 9: (a) Mean per-cell flash rate  $\bar{f}_c$  determined for LIS using the definitions of Table 1. Rates are *not* scaled for detection efficiency. Bar shading is as in Fig. 5. Total number of cells in each analysis region is shown at top. (b) Cumulative distribution function of  $f_c$ , full period, for land and ocean domains.

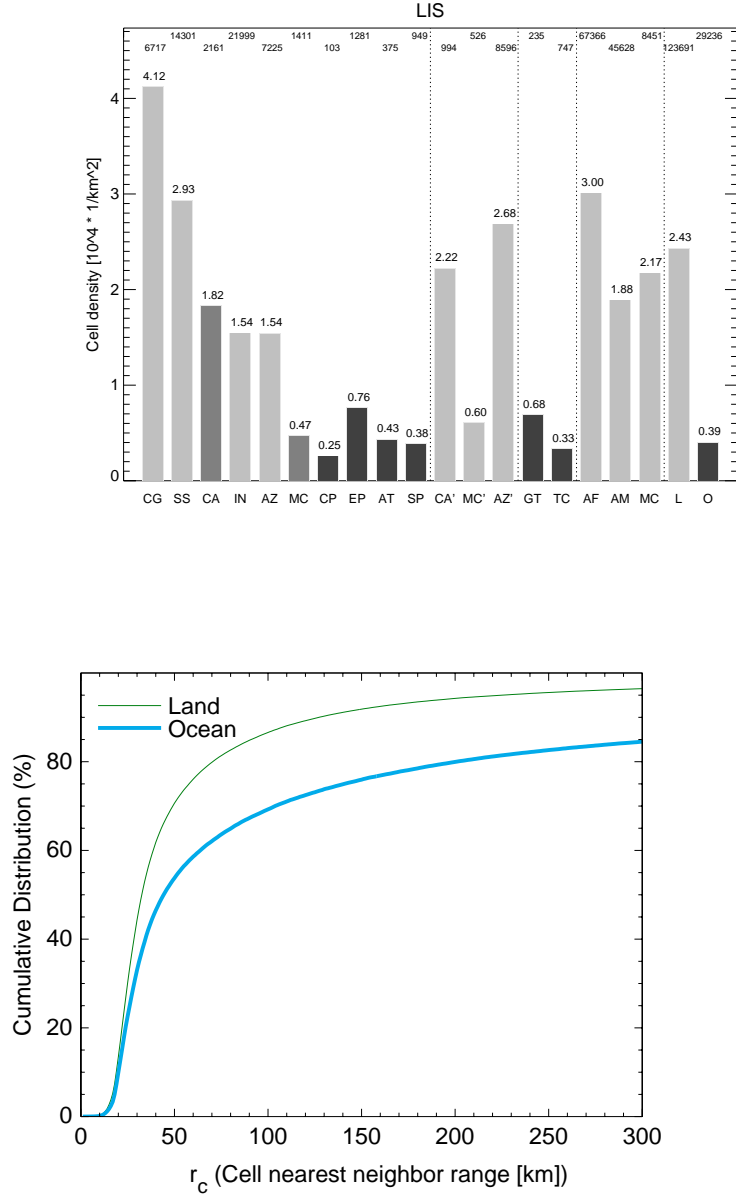


FIGURE 10: (a) Mean cell spatial density  $\bar{d}_c$  determined for LIS using the definitions of Table 1. Bar shading is as in Fig. 5. Total number of cells in each analysis region is shown at top. (b) Cumulative distribution function of  $r_c$  (cell nearest neighbor range), full period, for land and ocean domains.

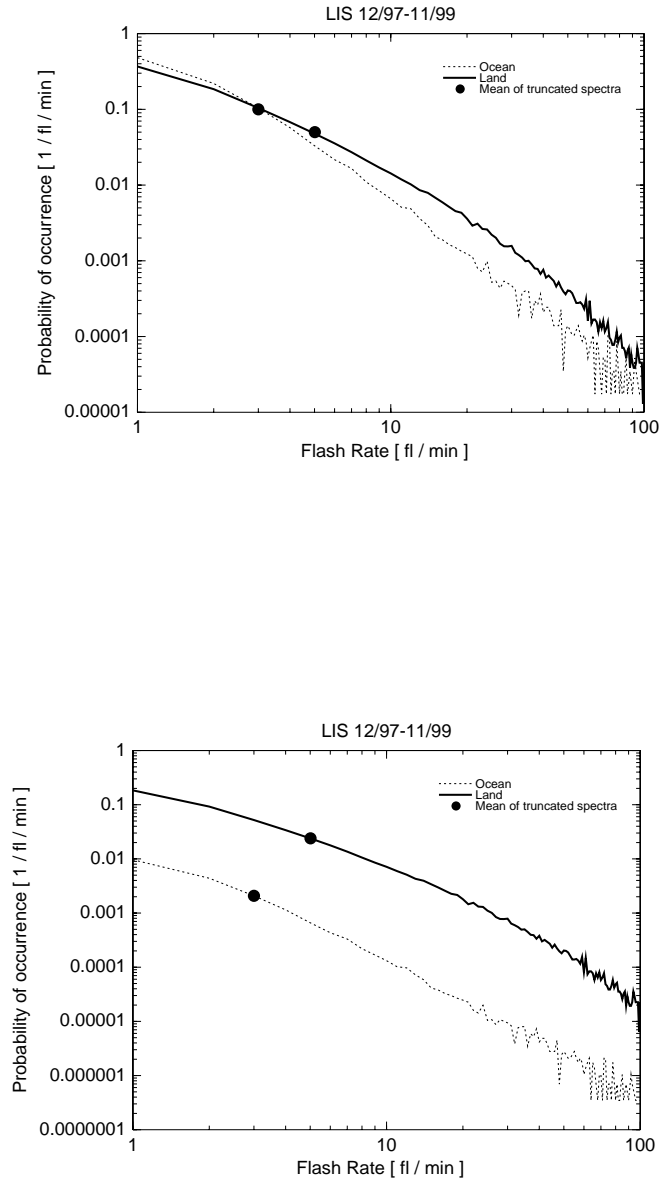


FIGURE 11: (a) Per-cell flash rate  $f_c$  spectra observed by LIS, land and ocean, assuming a 75%  $DE_f$ . The spectra of land and ocean  $f_c$  do not differ appreciably. (b) As in (a) but normalized by the results of Nesbitt et al (2000), who found that 50% and 98% of deep cells over land and ocean, respectively, were not observed to flash by LIS. The population of cells flashing at rates less than  $\sim 1$  fl/min is not yet determinable from these data.

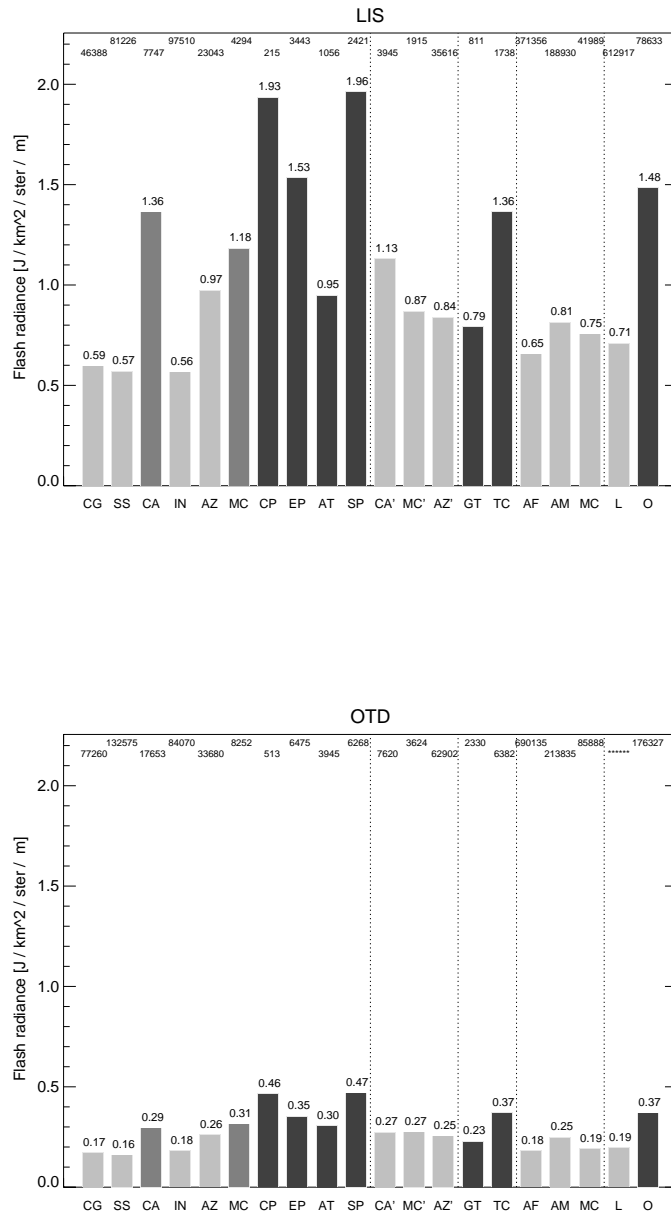


FIGURE 12: Mean flash radiance  $\bar{R}_f$  determined for OTD and LIS using the definitions of Table 1. Bar shading is as in Fig. 5. Total number of flashes in each analysis region is shown at top.



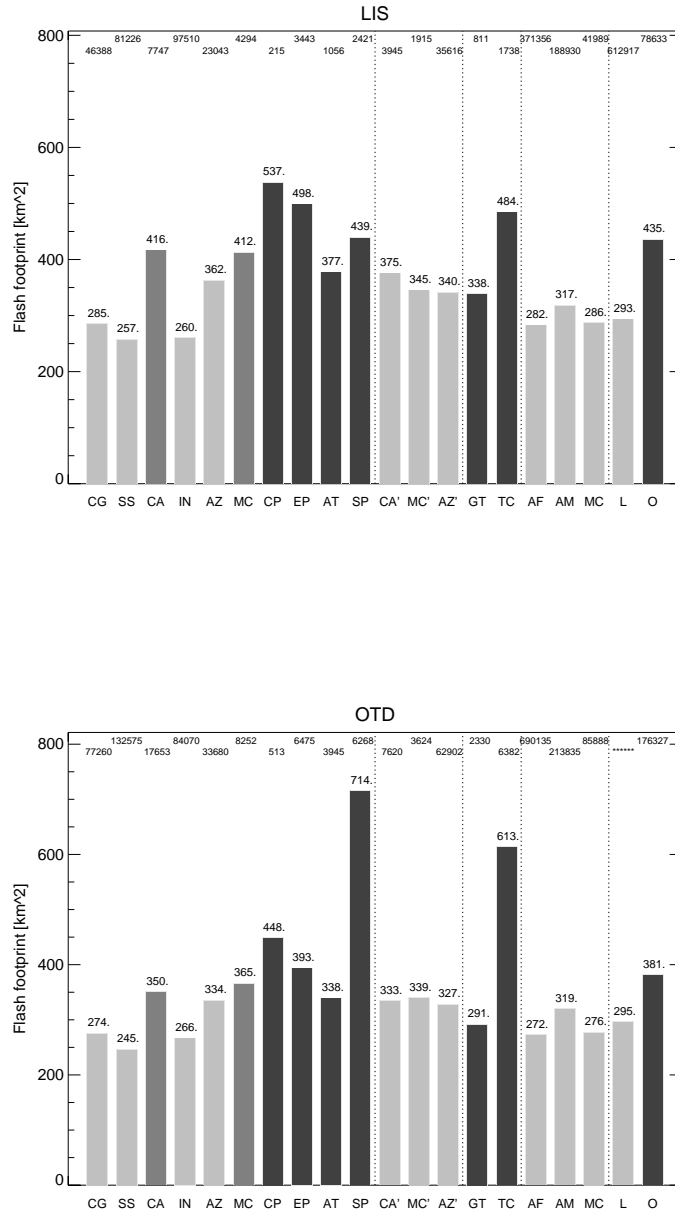


FIGURE 13: Mean flash footprint  $\bar{A}_f$  determined for OTD and LIS using the definitions of Table 1. Bar shading is as in Fig. 5. Total number of flashes in each analysis region is shown at top.

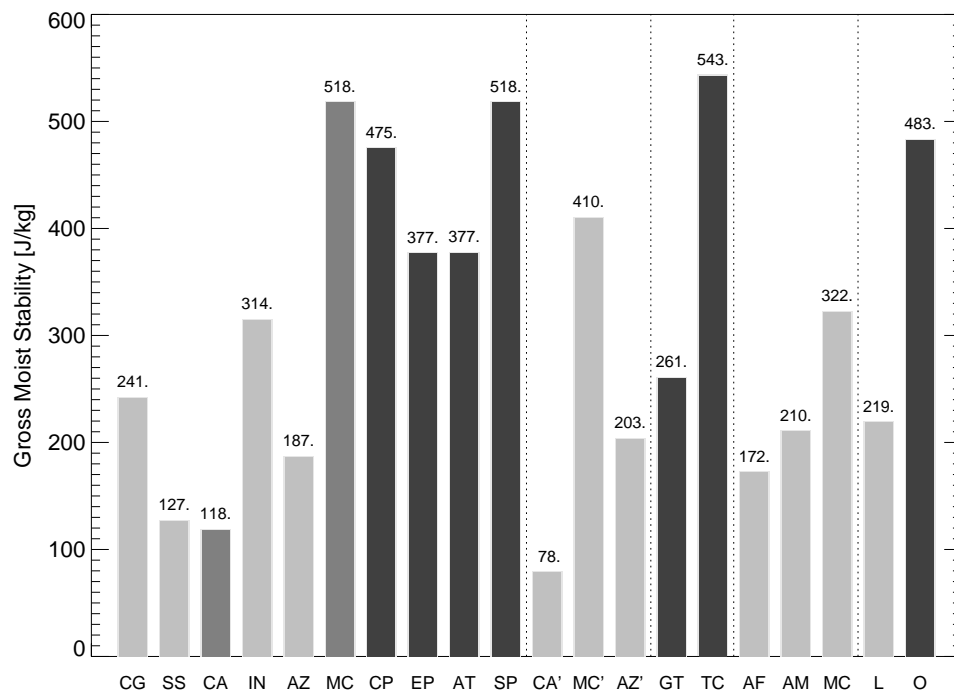


FIGURE 14: Gross moist stability  $M$  as computed by Yu et al (1998) for the subregions and subperiods of Table 1.

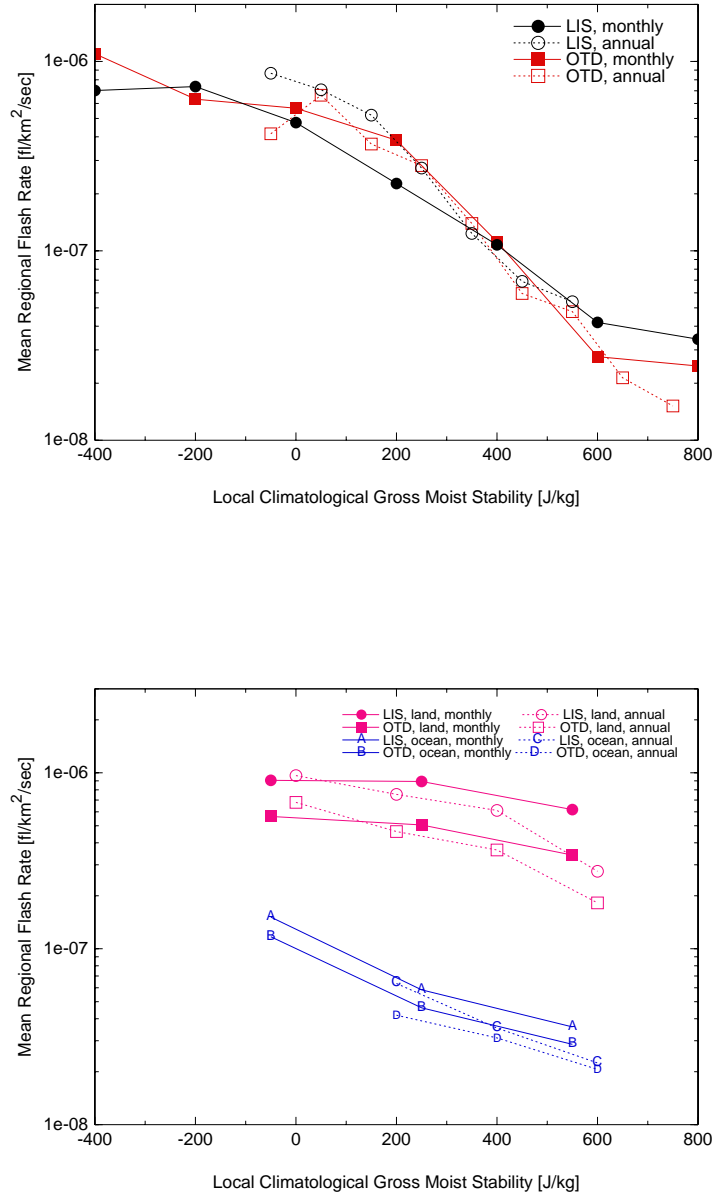


FIGURE 15: (a) Regional flash rate  $f_r$  vs gross moist stability  $M$ ; average of all 2.5x2.5 deg OTD and LIS locations within the Yu et al (1998) "continuously convective region" mask is presented for each  $M$ -bin. OTD and LIS data have been cross-normalized in this plot. (b) As in (a) but separated into contributions from land (upper) and ocean (lower) grid locations.

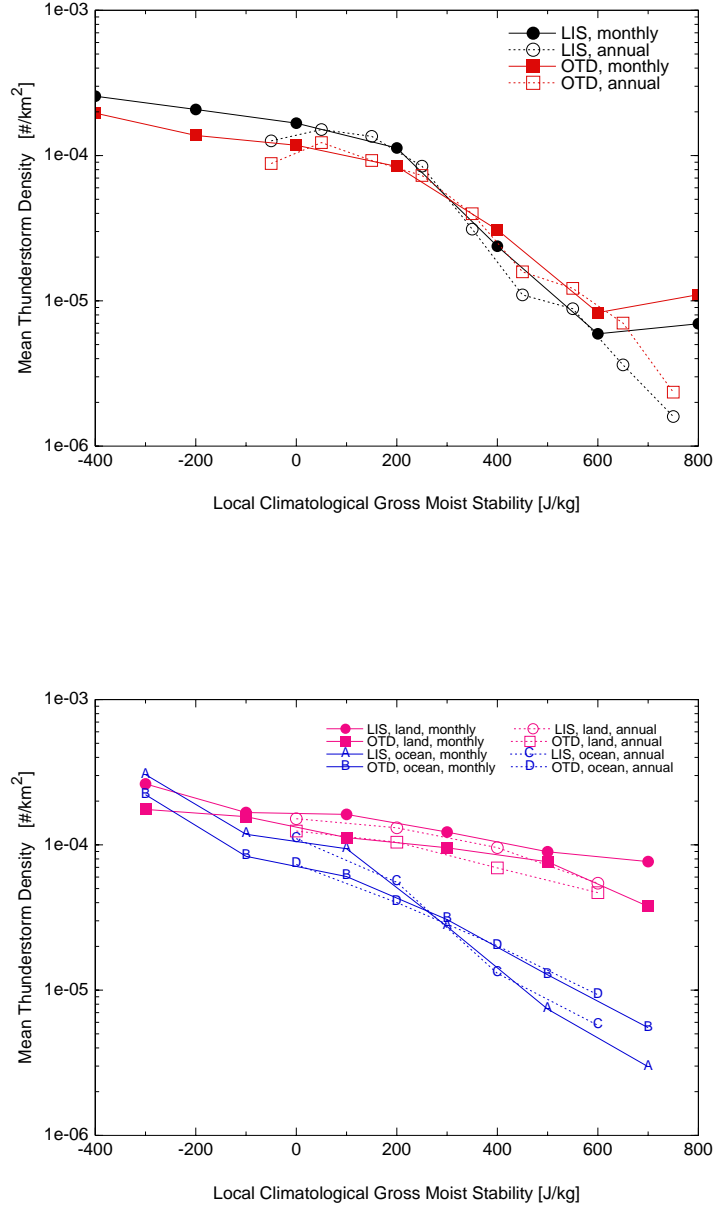


FIGURE 16: (a) Cell density  $d_c$  vs gross moist stability  $M$ ; average of all  $2.5 \times 2.5$  deg OTD and LIS locations within the Yu et al (1998) "continuously convective region" mask is presented for each  $M$ -bin. (b) As in (a) but separated into contributions from land (upper) and ocean (lower) grid locations.

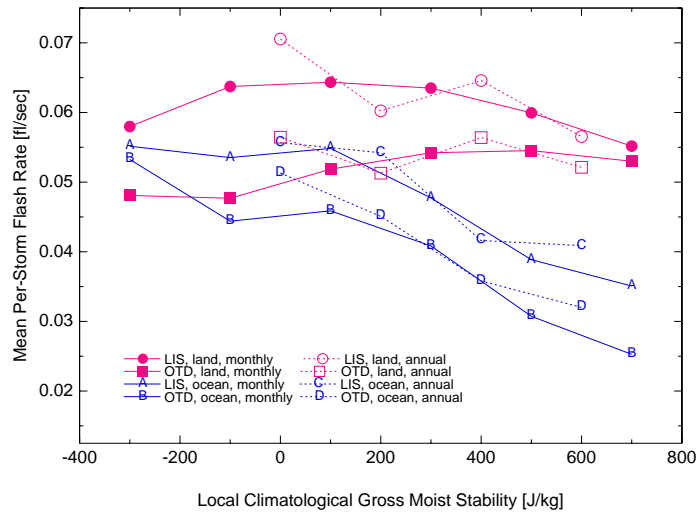
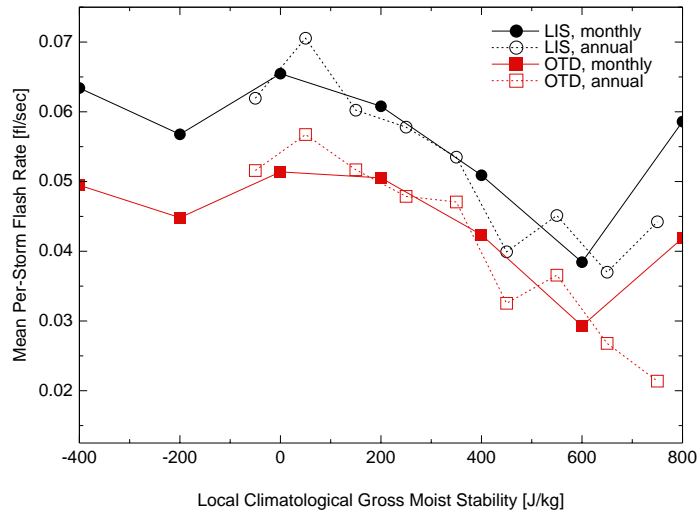


FIGURE 17: (a) Cell flash rate  $f_c$  vs gross moist stability  $M$ ; average of all  $2.5 \times 2.5$  deg OTD and LIS locations within the Yu et al (1998) "continuously convective region" mask is presented for each  $M$ -bin. (b) As in (a) but separated into contributions from land (upper) and ocean (lower) grid locations.

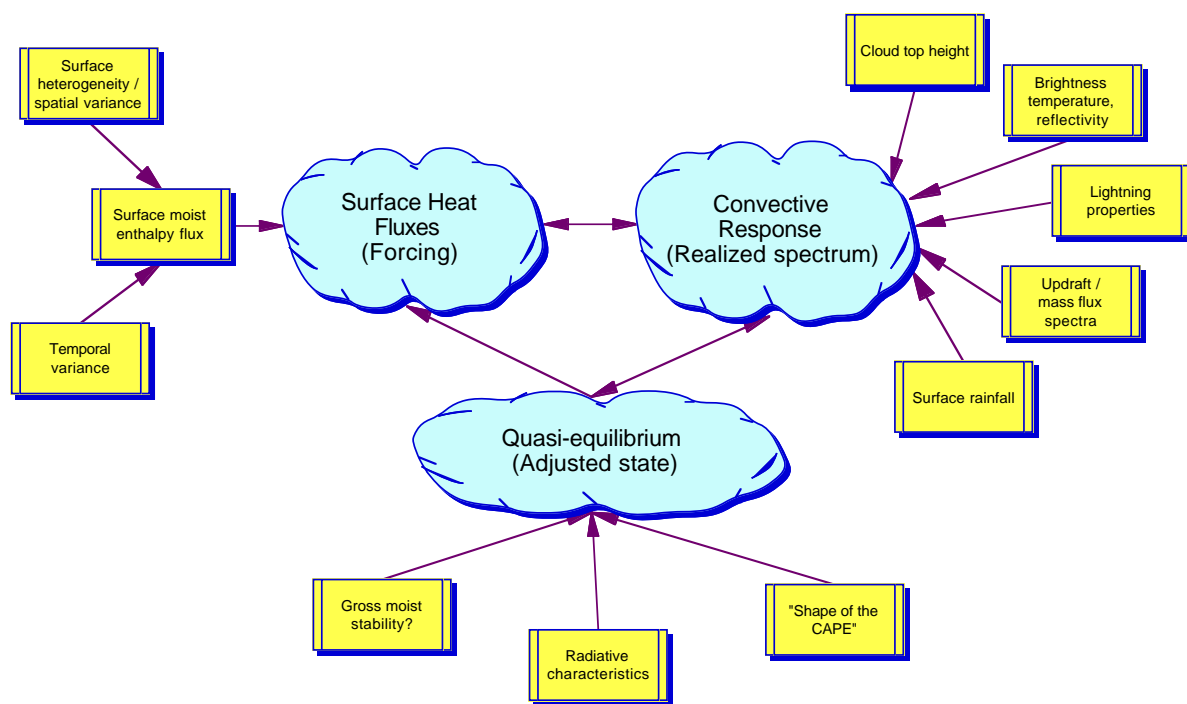


FIGURE 18: Conceptual diagram of controls needed to intercompare convective spectrum observations across different regions or "regimes".

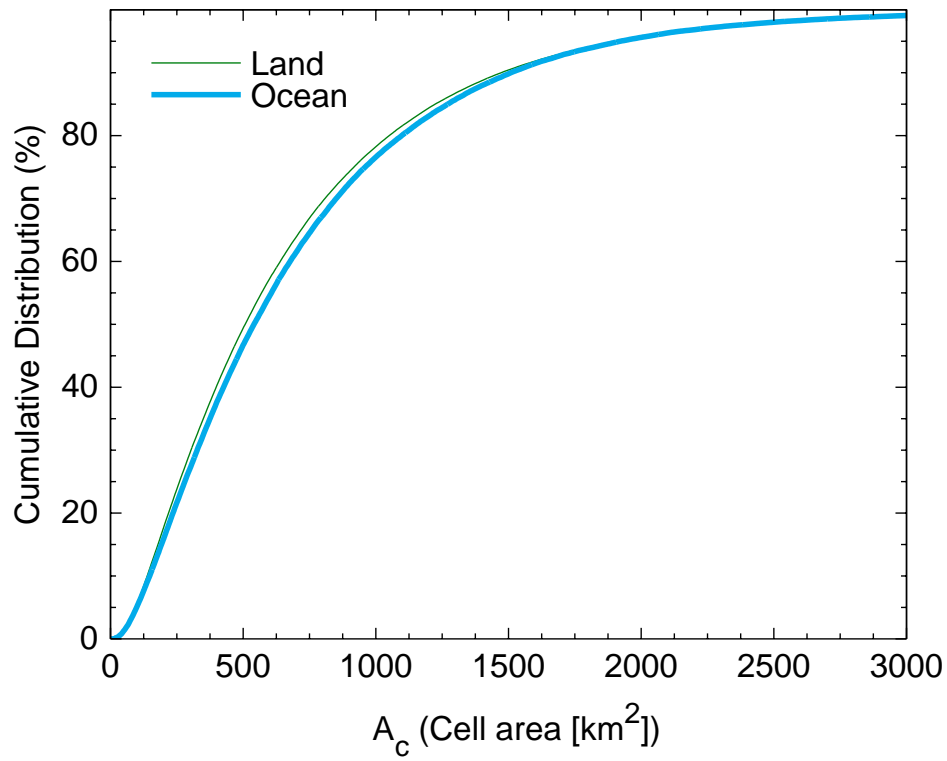


FIGURE 19: Cumulative distribution function of cell area  $A_c$  for land and ocean. Consistency of the distributions suggests that cell identification algorithms function comparably between land and ocean, and may not be biasing the resulting  $f_c$  and  $d_c$  distributions.